**Small-strain shear modulus and strength increase of cement-treated clay**

Technical Manuscript submitted for publication to the *Geotechnical Testing Journal*

Author 1 (Corresponding Author):

R. D. Verástegui Flores

Ph.D Student / Academic Assistant, Laboratory of Geotechnics, Ghent University, Belgium

Technologiepark 905, B-9052 Zwijnaarde, Belgium; Tel. +32 9 264 5725, Fax. +32 9 264 5849

Ramiro.VerasteguiFlores@UGent.be

Author 2:

G. Di Emidio

Ph.D Student / Academic Assistant, Laboratory of Geotechnics, Ghent University, Belgium

Technologiepark 905, B-9052 Zwijnaarde, Belgium; Tel. +32 9 264 5720, Fax. +32 9 264 5849

Gemmina.DiEmidio@UGent.be

Author 3:

W. F. Van Impe

Professor, Laboratory of Geotechnics, Ghent University, Belgium

Technologiepark 905, B-9052 Zwijnaarde, Belgium; Tel. +32 9 264 5717, Fax. +32 9 264 5849

William.VanImpe@UGent.be

**ABSTRACT**

A simple nondestructive technique was used as an alternative method to monitor the hardening of cement-treated clay as a function of time. The principle of this monitoring technique is based on the use of bender elements to measure the small-strain shear modulus ($G_0$) at various time intervals. The strength increase was monitored by conventional unconfined compression testing. Experimental work was carried out on Kaolin clay treated with Portland cement and blastfurnace slag cement at different dosages. The results showed that $G_0$, as well as strength, of cement-treated samples increases logarithmically with time. However, blastfurnace slag cement produces a slower hardening rate early after mixing. It was found that for each binder type, the $G_0$ increase and the strength increase, when normalized, follow a common trend. Such hardening function may be used as the basis of a strength prediction rule. The functions obtained are in good agreement with data on other cement-treated inorganic clays published in the literature.

**KEYWORDS**: soft soil, cement, compressive strength, small-strain shear modulus, bender elements.

## INTRODUCTION

Soft soils have always been of great concern in civil engineering due to their low strength and high compressibility. Over the years, many construction techniques and ground improvement methods have been developed to tackle those problems, for example: staged construction, preloading, enhanced drainage to accelerate consolidation, etc. The Deep Mixing method for ground improvement is an alternative to such techniques. The method can be classified as a permanent soil improvement technique with addition of cementing agents mixed in place. Nowadays, binders such as cement, quicklime, fly ash and blastfurnace slag are commonly used to enhance the mechanical properties of natural soft soil (Porbaha et al., 2000; EuroSoilStab, 2002; CDIT, 2002).

Although Deep Mixing has been in use worldwide for over three decades, only recently major research initiatives are being stimulated to study the behavior of soils treated with binders. The actual mechanism of improvement, interaction of binder-treated material with natural soils and its long-term behavior are topics still in need of research. This paper focuses on the mechanism of improvement of cement-treated clay.

Traditionally, the improvement effect of a binder is studied by measuring the compressive strength of cement-treated specimens at various curing times by unconfined compression testing. However, the amount of data obtained is often limited to a few curing times and is usually subjected to scatter.

In this paper, a nondestructive technique was used as an alternative method to monitor the hardening of cement-treated clay. The technique makes use of bender elements (Dyvik and Madshus, 1985) to measure the small-strain shear modulus ($G_0$) of a single sample at specific time intervals. This stiffness modulus is typically associated with small shear-strain levels of about $10^{-3}$% and below. In general, $G_0$ is governed by a number of factors such as stress history, stress level, void ratio, soil fabric and the stiffness of the soil skeleton, which is determined by interparticle contacts (Santamarina et al., 2001). Then, an increase of $G_0$ can be expected with increasing interparticle cementation.

Experimental work was carried out on cement-treated Kaolin clay using two types of binders at different dosages, Portland cement and blastfurnace slag cement. The results of monitoring confirmed an increase of $G_0$ with time during hydration of the cements. A series of unconfined compression tests was carried out simultaneously, showing a similar pattern for unconfined compressive strength (UCS). Monitoring of the small-strain shear modulus of cement-treated soils was shown to provide valuable additional information to study the hardening of these materials.

**BRIEF REVIEW OF PREVIOUS STUDIES**

The magnitude of strength increase in time of materials mixed with cementing agents has been a topic of investigation in concrete research for about 6 decades already. Neville (1995) and Carino (2001) present an overview of relationships that have been used to represent strength development. The early work of Plowman (1956) showed that compressive and tensile strengths of concrete plotted against the logarithm of time under isothermal conditions give a straight line. Out of his work, the first type of strength increase relationship was proposed:

$$S_T / S_0 = A + B \log(T) \qquad (1)$$

where $S_T$ is the strength at an age T, $S_0$ is a reference strength (for example at an age of 28 days) and A and B are constants.

Several improved versions and alternatives to the basic strength increase relationship have been introduced such as the hyperbolic equation (Eq. 2), the parabolic hyperbolic equation (Eq. 3) or the exponential equation (Eq. 4):

$$S = S_u \frac{k(t-t_0)}{1+k(t-t_0)} \qquad (2)$$

$$S = S_u \frac{\sqrt{(k(t-t_0)}}{1+\sqrt{k(t-t_0)}} \qquad (3)$$

$$S = S_u \, exp\left(\frac{-d}{\sqrt{t-t_0}}\right) \qquad (4)$$

where $S_u$ is an asymptotic value of strength, k is the rate constant and $t_0$ is the time at which strength development is assumed to begin (usually of the order of 0.15 days ).

Each of these relationships has its own limitations and ranges of applicability. Nevertheless, Neville (1995) states that the newer versions (Eq. 2-4) are indeed improvements but at the expense of introducing complications in the development and use of the functions; He also affirms that the original logarithmic function remains a useful tool for use in practice.

With the introduction of soil improvement methods with addition of binders, the study of strength development in time of cemented soils soon became relevant in geotechnical research as well. To the author's knowledge the first strength gain relationship for cemented soil was that proposed by Mitchell (1974):

$$UCS_{T2} = UCS_{T1} + K \log (T2/T1) \quad (5)$$

where $UCS_{T2}$ is the unconfined compressive strength at an age T2, $UCS_{T1}$ is the unconfined compressive strength at an age T1 and K is a constant.

Nagaraj and Miura (1996) conducted unconfined compressive tests on four inland clays treated with Portland cement at high water content and proposed the following relationship:

$$UCS_T / UCS_{14days} = a + b \ln(T) \quad (6)$$

where $UCS_T$ is the unconfined compressive strength at an age T, $UCS_{14days}$ is the 14-day unconfined compressive strength and a and b are constants. They reported values of a = -0.20 and b = 0.458 for those soils based on strength data with significant scatter.

Horpibulsuk et al. (2003), based on the work of Nagaraj and Miura (1996) and a larger database, but still with significant scatter, proposed the following relationship:

$$UCS_T / UCS_{28days} = a + b \ln(T) \quad (7)$$

The unavoidable scatter of strength data observed in the literature of concrete and geotechnical research is probably triggered by difficulties producing samples of repeatable quality. Therefore, the use of nondestructive techniques for monitoring hardening of cemented material got more attention recently. For example, Reinhardt and Grosse (2004) introduced a technique for the continuous monitoring of setting of concrete with ultrasonic waves.

Similarly, in geotechnical research, nondestructive testing of geomaterials by bender elements (Dyvik and Madshus, 1985) to determine the shear wave velocity and hence the small-strain shear modulus, $G_0$, has become common in the last decades. $G_0$ is a very valuable parameter as it is governed by factors such as stress history, stress level, void ratio, soil fabric and the stiffness of the soil skeleton. Then, it is not surprising that $G_0$ has been correlated to other soil properties like strength of artificially cemented soils. A reasonably linear correlation between $G_0$ and UCS has been reported in the literature (Tatsuoka et al., 1996; Hird and Chan, 2005; Van Impe et al., 2005; Lohani et al., 2006; Helinski et al., 2007). In most studies, $G_0$ was measured on samples by bender elements just before compression testing.

A bender element consists of a pair of piezoceramic plates bonded to a metal shim and to outer electrodes. Piezoceramics are materials that generate an electrical output when subjected to mechanical deformation or that bend when electrically excited. A pair of bender elements (located at opposite ends of a sample) is used for $G_0$ determination. One of the elements acts as shear wave transmitter and the other acts as the receiver. By measuring the travel time (t) of the shear wave through the sample, the shear wave velocity ($V_s$) can be determined as:

$$V_s = L / t \quad (8)$$

where L is the tip-to-tip distance between benders. Furthermore, the small-strain shear modulus $G_0$ is estimated through:

$$G_0 = \rho V_s^2 \quad (9)$$

where ρ is the bulk density of the sample.

This apparently simple method has been the subject of extensive research (e.g. Dyvik and Madshus, 1985; Brignoli et al., 1996; Arulnathan et al., 1998; Leong et al, 2005). Some issues regarding the bender elements installations and test execution have been summarized by Lee and Santamarina (2005). Furthermore, the various interpretation methods for evaluating the shear wave velocity (time-domain and frequency-domain based methods) and their limitations have been thoroughly discussed by Viana da Fonseca et al. (2009).

## MATERIALS

The materials used in this investigation were Kaolin clay, two types of cement, namely Portland cement and Blastfurnace slag cement, and water.

### KAOLIN CLAY

A commercial processed Kaolin clay (Rotoclay HB®, Goonvean, St. Austen, UK) was used in this investigation. The clay was available as a dry powder. Some physical properties of this material are summarized in table 1.

Scanning Electron Microscope (SEM) analysis was performed on this material. SEM is a type of electron microscope capable of producing high resolution images of a sample's surface at magnification levels that can go up to molecular levels. These images have a 3D appearance and may be useful for judging the microstructure of a sample. The working principle of SEM is simple: a beam of electrons is shot to a sample and as a result of their interaction, electrons and photons (e.g. X rays) from the sample are released. These electrons and photons are captured by detectors, providing valuable information for each point on the sample's surface. Just before microscopy, the samples were dried, subjected to vacuum for 12 hours and sputtered with gold coating. A SEM picture of the natural kaolin clay at a magnification of 2500x is shown in figure 1a. The picture shows that this material is homogeneous and that it is composed of agglomerates of clay particles. Kaolinite particles show pseudo-hexagonal sharp-edged plate shape. Figure 1b shows the results of a surface analysis of energy dispersive X-ray spectroscopy on the same sample. This analysis gives information about the chemical composition of the sample. Three main components can be clearly identified Aluminium (Al), Silicium (Si) and Oxigen (O) in agreement with the composition of the predominant mineral kaolinite $Al_2Si_2O_5(OH)_4$. However, also a small amount of Potassium (K) can be identified, probably because of the presence of traces of mica.

CEMENTS

Two types of cement were used: Portland cement and blastfurnace slag cement. Portland cement (CEM I 52.5 N) consists predominantly of Portland clinker while blastfurnace slag cement (CEM III/B 32.5 N LH HSR LA) consists of 65% to 80% of blastfurnace slag (a by-product of pig iron manufacture) and 20% to 35% of Portland clinker.

CEM I chosen here has a nominal strength of 52.5 MPa. On the other hand, CEM III/B has a nominal strength of 32.5MPa and shows low hydration heat (LH), high resistance against sulphates (HSR) and limited alkali content (LA).

WATER

Purified water of uniform quality was used for admixture of soil and cement. Before use, water was treated by a purifying system consisting of a series of filters including a deionization filter, reverse osmosis and UV filter. As a result, an electrical conductivity of EC < 2 μS/cm and a pH of about 8 were obtained.

## METHODS AND PROCEDURES

### SAMPLE PREPARATION

Although there is no unique standardized method of mixing cement and clay, it is possible to establish a common line based on current practice worldwide. The sample preparation method used here was based on various recommendations e.g. EuroSoilStab (2002), CDIT (2002) and Bhadriraju et al. (2008).

The sample preparation procedure was not meant to simulate actual conditions one may expect in actual ground improvement applications. Instead, the main goal of this procedure was to produce uniform and homogeneous samples. Samples were prepared for the two test types performed here, small-strain shear modulus testing (nondestructive) and unconfined compression testing. The small-strain testing requires a single sample which is contained in the testing setup and remains there throughout the whole testing period. On the other hand, unconfined compression testing requires the preparation of multiple cylindrical specimens. The specimens tested here have a diameter of 38 mm and a height of 86 mm in accordance with ASTM D2166-00.

The initial water content of the Kaolin clay was set to 2 times the liquid limit (w=115%) to represent a very soft soil. Furthermore, the cement dosage was fixed to 5%, 10% and 20% (in dry mass).

The laboratory equipment used for soil/cement mixing and sample preparation consisted of an industrial dough mixer, a weighing scale, a spatula, moisture tins, stainless-steel cylindrical moulds with a diameter of 38 mm and paraffin foil for sealing.

After weighing the appropriate amount of dry soil and binder, they were initially mixed dry in the dough mixer for about 2 minutes until a homogeneous binder distribution was observed. Next, the appropriate amount of water was weighed and incorporated in the mixing bowl. Mixing was extended for another 7 minutes approximately. The mixing was paused 1 or 2 times to remove soil attached to the walls of the mixing bowl. The mix at this point showed a liquid consistency and it was ready to be poured directly in the small-strain shear modulus testing setup or to be used in the manufacture of cylindrical specimens for unconfined compression testing.

Such specimens were cast in stainless-steel cylindrical molds (with a diameter of 38 mm and a height of 86 mm) lightly coated with vaseline on the inside. To avoid formation of large pores within the specimens, the molds were lightly shaken during the pouring process. The bottom and top ends of the molds were sealed with paraffin film and kitchen foil to prevent moisture loss in the mix. Next, the molds were stored in an air-conditioned room at 18°C and they were allowed to cure for 7 days. After that period, the specimens were carefully extruded out of the molds, they were wrapped in foil and once again stored in the air-conditioned room to resume curing until the testing day. Unconfined compression test specimens were allowed to cure for a period ranging from 7 days to 56 days in order to investigate the development of strength with time.

Out of the determination of parameters such as the water content and void ratio of cured specimens, it was found that the preparation procedure successfully produced samples of similar characteristics. Table 2 summarizes some statistics of measured water content and calculated void ratio of cemented specimens at a cement dosage of 20% after a curing period of 28 days. The data showed a normal distribution and limited scatter. The maximum standard deviation of void ratio was only 0.027 while the maximum standard deviation of water content was 1.08 (%).

Finally, a cement-treated sample was analyzed with the scanning electron microscope. The analyzed sample was treated with CEM I at a dosage of 20% and had a curing age of 28 days. A SEM picture at a magnification factor of 2500x is given in figure 2a. When comparing this picture to the untreated material, one can clearly notice a bonded structure with homogeneous texture where clay particles interact with cement hydration products. As a result of such interparticle cementation an increase of the small-strain shear modulus can be expected. Figure 2b shows the results of a surface analysis of energy dispersive X-ray spectroscopy. This analysis gives information about the chemical composition of the sample. Apart from the three main components of the natural Kaolin such as Al, Si and O, an extra peak in the spectrum can be observed which corresponds to Calcium (Ca), the main component of cement hydration products.

## SMALL-STRAIN SHEAR MODULUS TESTING

The small-strain shear modulus $G_0$ was evaluated by bender element testing. The bender elements used here are of the type T220-A4-203x (Piezo Systems, Inc.) with a length of 12 mm, a width of about 6 mm and a thickness of 0.5 mm. Series elements were used as transmitter and receiver. They were wired and coated with several layers of polyurethane varnish for water-proof protection. They were assembled into threaded brass fittings to simplify installation (Fig. 3a). The elements were anchored in the fittings by filling the gap with epoxy. To provide for grounding, a layer of conductive paint was placed around the bender plate and put in contact with the fitting (Fig. 3b) which was ground.

On top of that, a finishing layer of polyurethane varnish was placed for protection. The effective bender element length protruding out of the fitting was about 6 mm.

The design of the testing apparatus was based on the device developed by Reinhardt and Grosse (2004) for the evaluation of concrete setting, making use of ultrasonic waves. The apparatus proposed here for the monitoring of $G_0$ is illustrated in figure 4. It consists of two plexiglass plates (500 mm x 130 mm x 15 mm) that hold a U-shaped styrofoam mold with an open space for housing a cemented sample. The bender element transmitter and receiver are fixed to the plexiglass plates, one in front of the other and vertically aligned. All parts are held together by four sets of screws and nuts resting on rubber disks in an attempt to avoid wave propagation through the apparatus itself.

Testing was started immediately after a soil/cement mix was prepared. The mix was poured into the styrofoam mold and allowed to cure under a constant temperature of about T=18°C. During that period, measurements of $G_0$ were performed on a regular basis. In order to avoid drying, the sample was kept all the time under a thin layer of purified water.

The input S-wave was generated by 1 cycle of a sinusoidal electrical pulse. The sinusoidal pulse was generated with a Matlab script, originally as a sound signal. The sound signal was captured out of the sound card of the computer that produced a small voltage (up to 5V). This electrical pulse was amplified with a linear amplifier to reach a peak-to-peak amplitude of at least 40 V. Both the input and output signal were recorded in a HP 3562A Dynamic Signal Analyzer. Averaging of multiple measurements helped to eliminate unwanted noise.

Measurements were performed twice a day during the first couple of days, daily up to the first month and 2 to 3 times per week afterwards. The travel time of the shear wave was evaluated by identifying the first direct arrival from the output signal (Dyvik and Madshuis, 1985; Hird and Chan, 2008; Lee et al., 2008). Many trial measurements were performed at each time step looking for the most appropriate input signal frequency that produced the best possible output signal quality with negligible near field effect. In principle, high frequencies decrease near field effects and produce clearer first arrivals. At the very beginning of the monitoring, such optimal frequency was of the order of 7 kHz but as the sample gained stiffness the frequency was increased as well up to 14 kHz by the end of the monitoring activities. Figure 5 illustrates shear wave recordings during the first 28 days of monitoring for the clay sample mixed with CEM I at a dosage of 10%. As can be seen, the signals show little interference, which facilitated the evaluation of the first arrival.

### UNCONFINED COMPRESSION TESTING

The unconfined compression test is traditionally used in Deep Mixing practice to evaluate the improvement effect of binders in the laboratory. This test allows the determination of the unconfined compressive strength (UCS), which is the maximum vertical stress that a sample can sustain, using strain-controlled application of an axial load. The cemented samples were compressed at a deformation rate of 0.5 mm/min. Such rate was sufficient to bring the samples to failure within less than 15 minutes as specified by ASTM D2166-00.

## RESULTS

### SMALL-STRAIN SHEAR MODULUS

Monitoring of small-strain shear modulus ($G_0$) increase was performed for 6 types of soil/cement mixes. Samples were mixed with Portland cement (CEM I) and blastfurnace slag cement (CEM III/B). For each cement type, three dosage levels were used 5%, 10% and 20% (in dry weight).

Measurements of $G_0$ during cement hydration are illustrated in figures 6a and 6b for samples treated with Portland cement and blastfurnace slag cement, respectively. Overall, $G_0$ increases with time. As expected for Portland cement, the greatest increase occurred within the first month and afterward a less marked increase was recorded. Similarly, $G_0$ of samples treated with blastfurnace slag cement increases with time but following a different trend.

It is clear that the trends for each binder type at the three dosage levels share some similarities among them. Then, by introducing a normalizing parameter a common trend for each binder type could probably be expected. Figure 7 presents the results of all tests normalized by $G_{0(28d)}$, which is the evaluated small-strain shear modulus at a curing time of 28 days chosen here as a reference age. The figure shows that all normalized measurements ($G_0/G_{0(28d)}$) plot in a quite narrow range defining a very clear hardening trend for each type of binder. These results on cement-treated Kaolin clay suggest that for a given binder, regardless of the dosage, the small-strain stiffness development with time is essentially the same.

Moreover, figure 8 illustrates the same values of normalized small-strain shear modulus $G_0/G_{0(28d)}$ but this time plotted against the curing time in logarithmic scale. Based on data up to a curing time of 100 days, the small-strain stiffness development with time of Portland cement-treated Kaolin clay can be characterized with a well-defined logarithmic trend (Fig. 8a). A best-fitting operation gives the following relationship with a coefficient of determination $R^2$ of 0.98:

$$G_0/G_{0(28d)} = 0.2381 \ln(t)+0.2145 \qquad (10)$$

On the other hand, the normalized small-strain stiffness development with time for the sample treated with blastfurnace cement is not fully linear in the semi-logarithmic chart (Fig. 8b). Initially hardening takes place at a much slower rate, up to the fourth curing day approximately. From then on, the stiffness development shows a linear trend as well, which is slightly steeper (more pronounced) than that for Portland cement. These features of hardening are in full agreement with results of concrete research. Barnett et al. (2006) states that strength development of blastfurnace cement concrete is considerably slower under standard curing conditions than that of Portland cement concrete, although the long-term strength is higher for the same water–cement ratio. Based on data up to a curing period of about 80 days, two best-fitting relationships were evaluated for cemented Kaolin clay. The first one is an exponential function ($R^2$=0.96) valid up to the fourth day of curing. The second one is a logarithmic function ($R^2$=0.98) valid for curing times beyond the fourth day. The best-fitting relationships for small-strain stiffness development under blastfurnace slag cement treatment are:

$$G_0/G_{0(28d)} = 0.0472\, t^{1.2866} \quad \text{(for } 0 < t < 4 \text{ days)} \qquad (11)$$

$$G_0/G_{0(28d)} = 0.3586 \ln(t)-0.2159 \quad \text{(for } t > 4 \text{ days)} \qquad (12)$$

The spreading of measurement points around the proposed best-fitting functions is quite limited. This suggests that the observed trends of normalized small-strain stiffness increase during cement hydration are indeed representative for each type of binder.

## UNCONFINED COMPRESSIVE STRENGTH

To investigate the strength increase of cement-treated Kaolin clay, unconfined compression tests were performed at 7, 14, 28, 42 and 56 days after mixing. At each curing time, two specimens were tested. Three types of soil/cement mixes were studied here: Kaolin clay mixed with Portland cement (CEM I) at a dosage of 10% and 20% and Kaolin clay mixed with blastfurnace slag cement (CEM III/B) at a dosage of 20%.

The results are summarized in figures 9a and 9b for samples treated with Portland cement and blastfurnace slag cement respectively. Overall, the unconfined compressive strength (UCS) increases with time. Similar to $G_0$ measurements, the strength of samples treated with Portland cement showed the greatest increase within the first month. The 28-day compressive strength of samples treated at 20% and 10% dosage was in the order of UCS ≈ 300 kPa and UCS ≈ 100 kPa respectively. This strength was observed to increase very little beyond 28 days of curing.

Samples treated with blastfurnace slag cement were mixed at a single dosage level of 20% (Fig. 9b). The results of strength measurement in this case show a more gradual increase. The compressive strength recorded higher values than Portland-cement treated samples at the same dosage. In fact, the 28-day compressive strength reached UCS ≈ 650 kPa and furthermore, the strength increase beyond 28 days of curing seems more pronounced.

## SMALL-STRAIN SHEAR MODULUS VERSUS COMPRESSIVE STRENGTH

Similar to $G_0$ data, the unconfined compressive strength was normalized with respect to the 28-day strength $UCS_{(28d)}$. Figure 10 compares normalized $G_0$ with normalized UCS of samples treated with both binders. Although there is some unavoidable scatter, especially for samples treated with Portland cement, the figure shows good agreement between $G_0/G_{0(28d)}$ and $UCS/UCS_{(28d)}$. These results suggest that the small-strain stiffness increase and the strength increase are closely related and follow similar trends, at least within the age range considered here. This would mean that the relationships relating $G_0/G_{0(28d)}$ with time (Eq. 10-12) could also be used (with enough accuracy) to describe the progress of UCS of cemented Kaolin with time, e.g. to predict the compressive strength (at any curing time) out of a single measurement of UCS at a specific curing time.

The stiffness/strength increase relationships proposed for cemented Kaolin clay were compared to strength increase data of other cement-treated soils reported in the literature (Porbaha et al., 2000; Horpibulsuk et al., 2003; Liu et al., 2008). In figure 11a, the strength increase with age of Black clays, Yangtze river clays and Bangkok clay treated with Portland cement (CEM I) is compared to the stiffness/strength increase function given by equation 10. Overall, a good agreement was found for all soil types, especially during the first month. After that, some scatter is observed.

Figure 11b illustrates strength increase data of Tokyo Bay clay and Kyushu Island clay treated with blastfurnace slag cement (CEM III/B). Porbaha et al. (2000) reported the compressive strength measurements on those samples as a function of time. At first sight, the strength increase on both soil types seems different. In fact, based on visual comparison, Porbaha et al. (2000) concluded that the improvement effect of blastfurnace slag cement is different for various soil types and that there is not a general trend in the improvement effect. However, if the results are normalized with respect to $UCS_{(28d)}$, we see that all points closely follow a common trend. Moreover, such trend shows excellent agreement with the hardening functions (Eq. 11 and 12) determined from Kaolin clay testing.

The stiffness/strength increase relationships were also compared with long-term strength gain data of stabilized soils (Topolnicki, 2004). Data of a deep marine clay stabilized with Portland cement shows a compressive strength ratio $UCS_{20years}$ / $UCS_{90days}$ of 2.2. Using equation 10, a ratio $UCS_{20years}/UCS_{90days}$ = 2.1 can be evaluated. Data on volcanic soil stabilized with blastfurnace cement shows a compressive strength ratio $UCS_{17years}/UCS_{28days} \geq 3$. Using equation 12, a ratio $UCS_{20years}$ / $UCS_{90days}$ = 2.92 can be evaluated. Again, here an satisfactory agreement was found.

These observations suggest that the hardening functions determined for Portland cement and blastfurnace slag cement treatment on Kaolin clay (Eq. 10, 11 and 12) are able to successfully describe the improvement effect of these binders on other natural soils as well, as long as large amounts of agents known to disrupt cement hydration (e.g. humic acids or sulphates) are not present in the soil or pore water.

**CONCLUSIONS**

A simple testing setup was developed to monitor the hardening of cement-treated Kaolin clay in time. The principle of this nondestructive monitoring technique is based on the use on bender elements to measure the small-strain shear modulus $G_0$ of a single cement-treated sample at specific time intervals. This procedure is proposed as an alternative to traditional unconfined compression strength (UCS) measurement.

Out of results on Kaolin clay mixed with Portland cement and blastfurnace slag cement at different dosages, it was found that $G_0$ increase and UCS increase of cement-treated soil are closely related. Introducing normalizing parameters such as $G_{0(28d)}$ and $UCS_{(28d)}$, which are the evaluated $G_0$ and UCS at a curing time of 28 days respectively, it was observed that $G_0/G_{0(28d)}$ and $UCS/UCS_{(28d)}$ follow essentially the same trend. That implies that a relationship relating $G_0/G_{0(28d)}$ with time could also be used to describe the progress of $UCS/UCS_{(28d)}$ of cemented Kaolin, e.g. to predict the compressive strength (at any curing time) out of a single measurement of UCS at a specific curing time.

The improvement effect of Portland cement on Kaolin clay could be fully described by a single logarithmic function of time. On the other hand, the improvement effect of blastfurnace slag cement shows slower hardening early after mixing (during the first four days approximately) followed by a slightly faster rate of hardening. Then, two functions were proposed, an exponential function for early hardening and a steeper logarithmic function of time for late hardening. These functions, evaluated on the basis of $G_0$ measurements on cemented Kaolin clay, show good agreement with UCS measurements.

Furthermore, the proposed hardening functions were compared to strength increase measurements of other cement-treated soils reported in the literature. Again, a good agreement was found. These results suggest that the hardening functions determined for Portland cement and blastfurnace slag cement treatment on Kaolin clay are able to successfully describe the improvement effect of these binders on other natural soils as well, as long as large amounts of agents known to disrupt cement hydration (e.g. humic acids or sulphates) are not present in the soil or pore water.

Monitoring of $G_0$ during hardening of cement-treated soil could be useful to aid the design of ground improvement. Moreover, the proposed technique could help to reduce the number of unconfined compression tests (traditionally carried out to study the impact of a binder) or to provide a clearer overview of stiffness/strength increase of cemented soil as it is less prone to scatter.

**ACKNOWLEDGMENTS**

The first author acknowledges the Department of Civil Engineering at Ghent University for financial support. The authors acknowledge D. Snoeck and P. Pollet for the help provided throughout this research.

**REFERENCES**

Arulnathan, R., Boulanger, R.W. and Riemer, M.F., 1998, "Analysis of bender element tests", *Geotechnical Testing Journal,* Vol. 21, No. 2, pp. 120–131.

ASTM Standard D2166-00: Standard Test Method for Unconfined Compressive Strength of Cohesive Soil, *Annual Book of ASTM Standards*, ASTM International, West Conshohocken, PA, 2000.

Barnett, S.J., Soutsos, M.N., Millard, S.G., Bungey, J.H., 2006, "Strength development of mortars containing ground granulated blast-furnace slag: Effect of curing temperature and determination of apparent activation energies", *Cement and Concrete Research,* Vol. 36, No. 3, pp. 434-440.

Bhadriraju, V., Puppala, A., Madhyannapu, R. and Williammee, R., 2008, "Laboratory procedure to obtain well-mixed soil binder samples of medium stiff to stiff expansive clayey soil for Deep Soil Mixing simulation", *Geotechnical Testing Journal,* Vol. 31, No. 3, pp. 225–238.

Brignoli, E.G.M., Gotti, M., Stokoe II, K.H., 1996, "Measurement of shear waves in laboratory specimens by means of piezoelectric transducers", *Geotechnical Testing Journal,* Vol. 19, No. 4, pp. 384–397.

Carino, N.J., 2001, "The maturity method: from theory to application", *Proceedings of the 2001 Structures Congress & Exposition,* Washington D.C., ASCE, pp. 1–18.

Coastal Development Institute of Technology (CDIT), 2002, *The Deep Mixing method: Principle, Design and Construction*. A.A. Balkema, The Netherlands.

Dyvik, R. and Madshus, C., 1985, "Laboratory measurements of $G_{max}$ using bender elements", *Proceedings of Conference on Advances in the Art of Testing Soils Under Cyclic Conditions*, Detroit, pp. 186–196.

EuroSoilStab, 2002, *Development of design and construction methods to stabilize soft organic soils: Design Guide Soft Soil Stabilization*, CT97-0351, European Project No.: BE 96-3177.

Helinski, M., Fahey, M., and Fourie, A., 2007, "Numerical modeling of cemented mine backfill deposition", *Journal of Geotechnical and Geoenvironmental Engineering,* ASCE, Vol. 133, No. 10, pp. 1308–1319.

Hird, C. and Chan, C.M., 2005, "Correlation of shear wave velocity with unconfined compressive strength of cement-stabilized clay", *Proceedings of International Conference on Deep Mixing Best Practice and Recent Advances*, Stockholm, pp. 79–85.

Hird, C., and Chan, C.M., 2008, "One-dimensional compression tests on stabilized clays incorporating shear wave velocity measurements", *Geotechnical Testing Journal,* ASTM, Vol. 31, No. 2, pp. 166-174.

Horpibulsuk, S., Miura, N. and Nagaraj, T., 2003, "Assessment of strength development in cement-admixed high water content clays with Abrams' law as a basis", *Geotechnique,* Vol. 53, No. 4, pp. 439–444.

Lee, C., Lee, J.S., Lee, W. and Cho, T.H., 2008, "Experiment setup for shear wave and electrical resistance measurements in an oedometer", *Geotechnical Testing Journal,* ASTM, Vol. 31, No. 2, pp. 149-156.

Lee, J. and Santamarina, J., 2005, "Bender elements: Performance and signal interpretation", *Journal of Geotechnical and Geoenvironmental Engineering*, ASCE, Vol. 131, No. 9, pp. 1063–1070.

Leong, E.C., Yeo, S.H. and Rahardjo, H., 2005, "Measuring shear wave velocity using bender elements", *Geotechnical Testing Journal,* ASTM, Vol. 28, No. 5, pp. 488-498.

Lohani, T., Tatsuoka, F., Tateyama, M. and Shibuya, S., 2006, "Strengthening of Weakly-Cemented Gravelly Soil with Curing Period", *Soil Stress-Strain Behavior: Measurement, Modeling and Analysis*, Geotechnical Symposium in Rome, pp. 455-462.

Liu, S., Zhang, D., Liu, Z. and Deng, Y., 2008, "Assessment of unconfined compressive strength of cement stabilized marine clay", *Marine Georesources and Geotechnology*, Vol. 26, pp. 19–35.

Mazzieri, F., Van Impe, P., Van Impe, W. and Constales, D, 2002, "Effect of consolidation on contaminant transport parameters of compacted clays", *Proc. of 4th Int. Congress on Environmental Geotechnics, ICEG*, Rio de Janeiro, pp. 183-188.

Mitchell, J.K., Veng, T.S. and Monismith, C.L.. 1974. "Behavior of Stabilized Soils under Repeated Loading". *In Performance Evaluation of Cement-Stabilized Soil Layers and Its Relationship to Pavement Design*. Department of Civil Engineering, University of California, Berkeley, California.

Nagaraj, T.S. and Miura, N., 1996. "Induced cementation of soft ground – A parametric assessment". *Proc. International Symposium on Lowland Technology*, Saga Univ., Japan, pp. 85–97.

Neville, A.M., 1995, *Properties of concrete*. Prentice Hall.

Plowman J.M., 1956, "Maturity and the strength of concrete", *Concrete Research, Vol. 8, No. 22, pp. 13-22.*

Porbaha, A., Shibuya, S. and Kishida, T., 2000, "State of the art in Deep Mixing technology, part III: Geomaterial Characterization", *Ground Improvement*, Vol. 4, No. 3, pp. 91–110.

Reinhardt, H. and Grosse, C., 2004, "Continuous monitoring of setting and hardening of mortar and concrete", *Construction and building materials*, Vol. 18, No. 3, pp. 145–154.

Santamarina, J., Klein, K. and Fam, A. (2001). *Soils and waves: particulate materials behaviour, characterization and process monitoring*, John Wiley and Sons, LTD.

Tatsuoka, F., Kohata, Y., Uchida, K. and Imai, K., 1996, “Deformations and strength characteristics of cement-treated soils in Trans-Tokyo Bay Highway Project”, *Proceedings of Grouting and Deep Mixing,* Balkema, Rotterdam, Vol. 1, pp. 453-459.

Topolnicki, M., 2004, “In situ soil mixing”, *In Ground Improvement, 2$^{nd}$ Edition, Moseley & Kirsch (Eds.),* Spon Press.

Van Impe, W.F., Verástegui Flores, R.D., Mengé, P., Van den Broeck, M., 2005, “Considerations on laboratory test results of cement stabilized sludge”. *In Proceedings of the International Conference on Deep Mixing: Best Practice and Recent Advances*, Stockholm, Sweden, pp. 163-168.

Viana da Fonseca, A., Ferreira, C. and Fahey, M., 2009, “A framework interpreting bender element tests, combining time-domain and frequency-domain methods”, *Geotechnical Testing Journal,* ASTM, Vol. 32, No. 2, pp. 91-107.

TABLE 1. Physical properties of Kaolin clay (Mazzieri et al., 2002)

| *Property* | *Value* |
|---|---|
| Specific gravity | 2.65 |
| Liquid limit, % | 57.7 |
| Plasticity Index | 28.6 |
| Activity | 0.7 |
| Silt size content, % | 59.6 |
| Clay size content, % | 40.4 |
| pH (4+1 extract) | 4.5 |
| EC (4+1 extract), μS/cm | 318 |

TABLE 2. Statistics of physical indexes of cemented specimens after a curing period of 28 days

| *Index* | *Binder type* | |
|---|---|---|
| | CEM I (20%) | CEM III/B (20%) |
| No. specimens | 18 | 18 |
| Void ratio | | |
| Mean | 2.50 | 2.55 |
| Std. deviation | 0.027 | 0.012 |
| Water content (%) | | |
| Mean | 88.6 | 90.6 |
| Std. deviation | 1.08 | 0.33 |

FIGURE CAPTIONS

Figure 1. SEM analysis of natural Kaolin clay: (a) picture at a magnification of 2500x (b) chemical composition out of EDS (energy dispersive spectrum)

Figure 2. SEM analysis of CEM I treated clay after 28 days curing: (a) picture at a magnification of 2500x (b) chemical composition out of EDS (energy dispersive spectrum)

Figure 3. Bender elements: (a) assembly in a brass fitting (b) detail of assembly

Figure 4. Small-strain shear modulus ($G_0$) monitoring setup: (a) side view (b) plan view

Figure 5. Shear wave signals collected during hardening of Kaolin clay mixed with CEM I at 10% over a period of 28 days.

Figure 6. $G_0$ measurements during cement hydration: (a) sample treated with Portland cement (b) sample treated with blastfurnace slag cement

Figure 7. Normalized shear modulus $G_0/G_{0(28\ days)}$ during cement hydration: (a) sample treated with Portland cement (b) sample treated with blastfurnace slag cement

Figure 8. $G_0/G_{0(28\ days)}$ vs. curing time in log. scale: (a) sample treated with Portland cement (b) sample treated with blastfurnace slag cement

Figure 9. Unconfined compressive strength: (a) sample treated with Portland cement (b) sample treated with blastfurnace slag cement

Figure 10. Correlation between normalized G0 versus normalized UCS: (a) sample treated with Portland cement (b) sample treated with blastfurnace slag cement

Figure 11. Comparison of the proposed hardening correlations for Kaolin clay to other soils from the literature: (a) sample treated with Portland cement (b) sample treated with blastfurnace slag cement

FIGURE 1

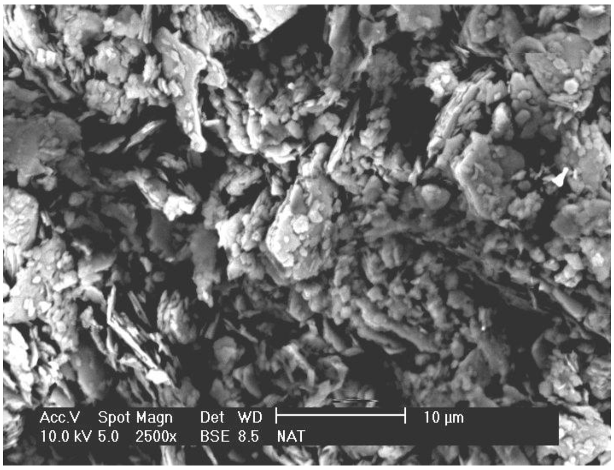
Acc.V Spot Magn Det WD 10 µm
10.0 kV 5.0 2500x BSE 8.5 NAT

(a)

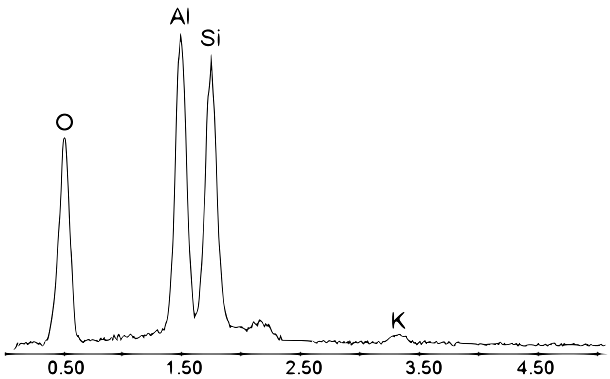
Al
Si
O
K
0.50
1.50
2.50
3.50
4.50

(b)

FIGURE 2

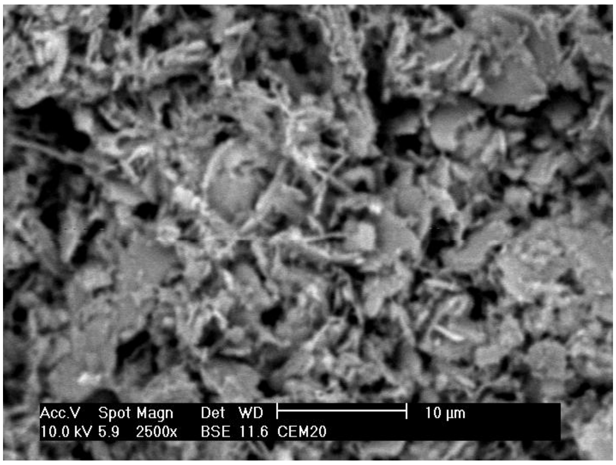
Acc.V Spot Magn Det WD 10 µm
10.0 kV 5.9 2500x BSE 11.6 CEM20

(a)

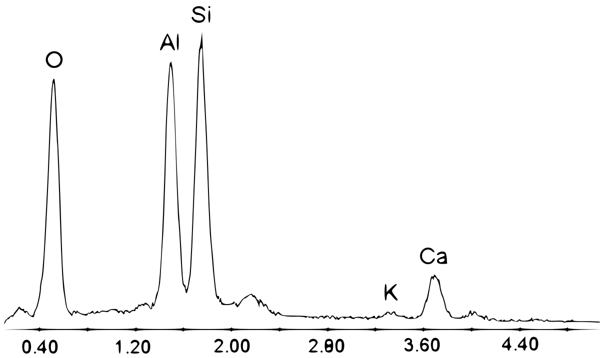
O
Al
Si
K
Ca
0.40
1.20
2.00
2.80
3.60
4.40

(b)

FIGURE 3

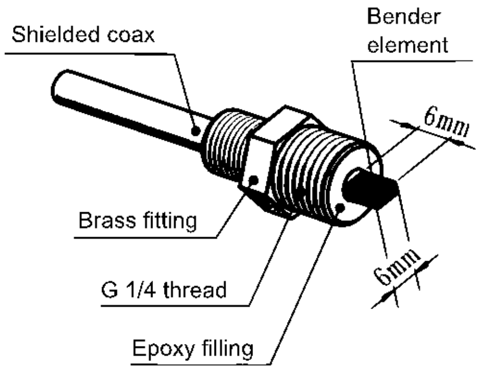
Shielded coax
Bender element
6mm
Brass fitting
6mm
G 1/4 thread
Epoxy filling

(a)

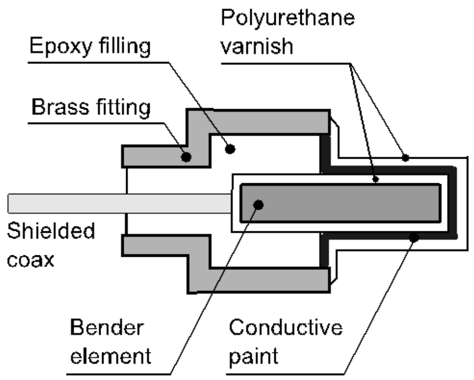
Polyurethane varnish
Epoxy filling
Brass fitting
Shielded coax
Bender element
Conductive paint

(b)

FIGURE 4

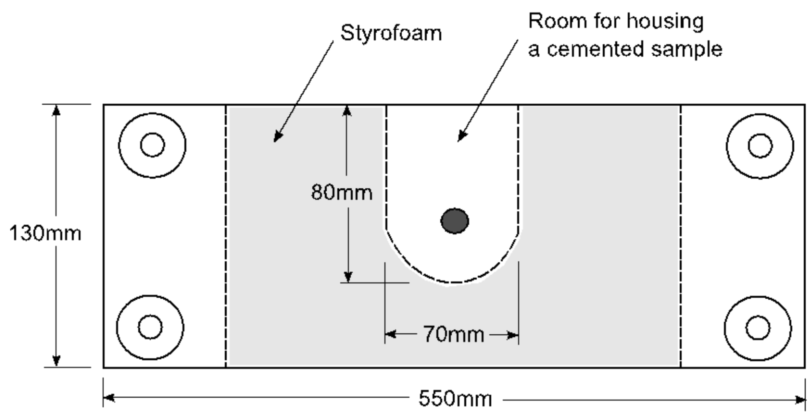
Styrofoam
Room for housing
a cemented sample
80mm
130mm
70mm
550mm

(a)

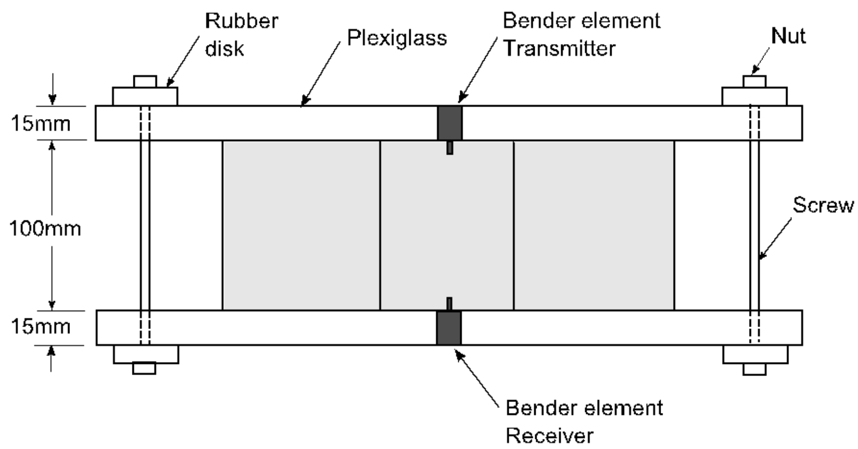
Rubber
disk
Plexiglass
Bender element
Transmitter
Nut
15mm
100mm
15mm
Screw
Bender element
Receiver

(b)

FIGURE 5

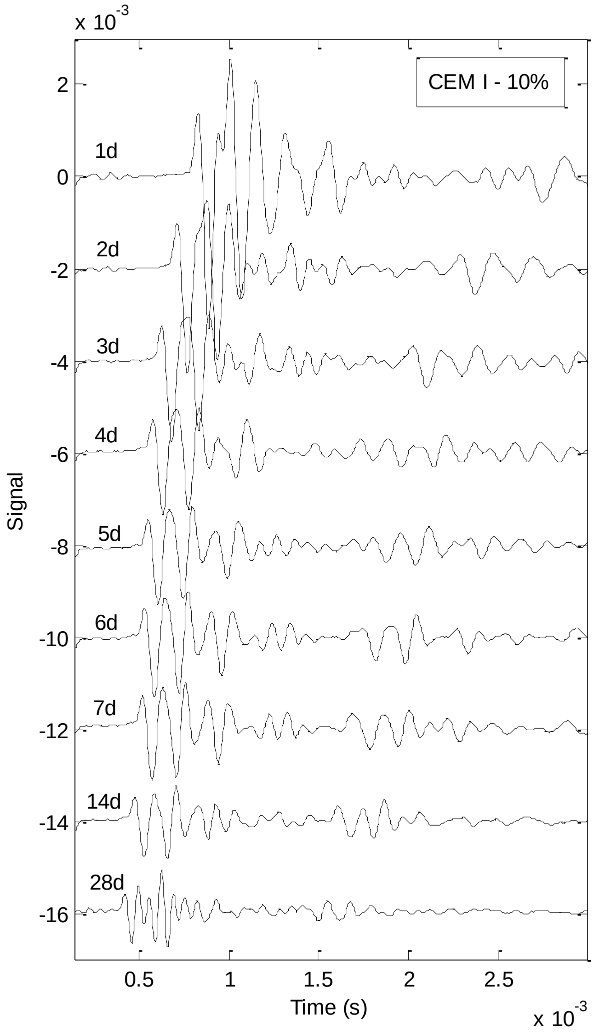

x 10^-3
CEM I - 10%
1d
2d
3d
4d
5d
6d
7d
14d
28d
2
0
-2
-4
-6
-8
-10
-12
-14
-16
Signal
0.5
1
1.5
2
2.5
Time (s)
x 10^-3

FIGURE 6

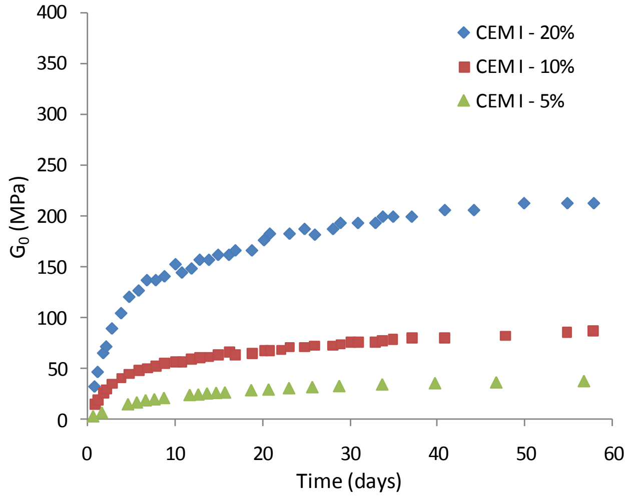

400
350
300
250
200
150
100
50
0
$G_0$ (MPa)
CEM I - 20%
CEM I - 10%
CEM I - 5%
0
10
20
30
40
50
60
Time (days)


(a)

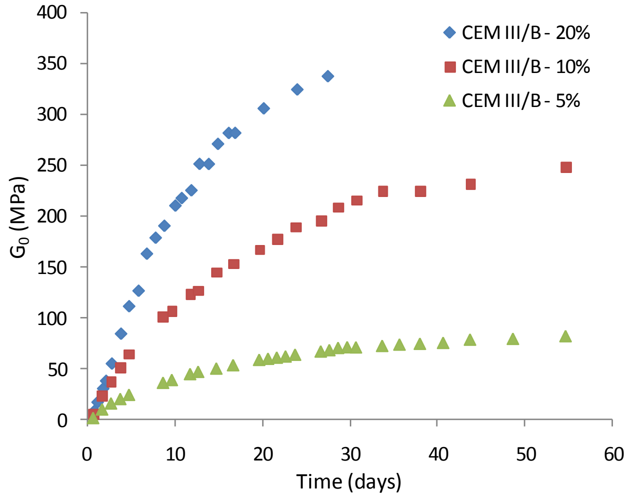

400
350
300
250
200
150
100
50
0
$G_0$ (MPa)
CEM III/B - 20%
CEM III/B - 10%
CEM III/B - 5%
0
10
20
30
40
50
60
Time (days)


(b)

FIGURE 7

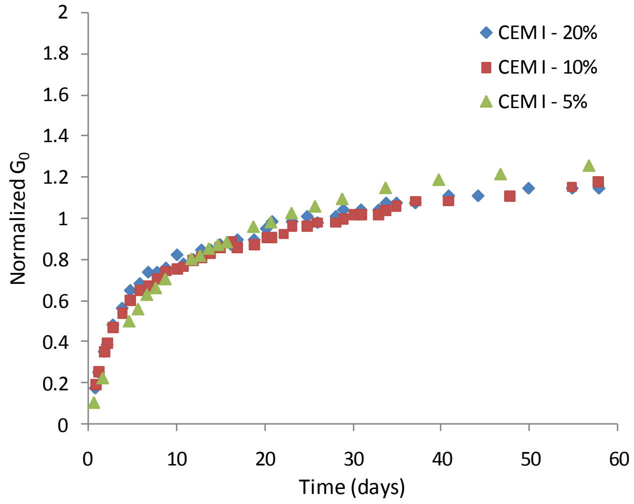

CEM I - 20%
CEM I - 10%
CEM I - 5%
Normalized G0
Time (days)


(a)

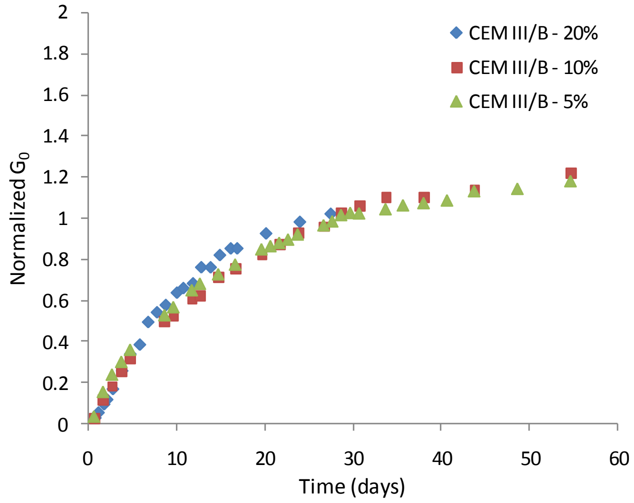

CEM III/B - 20%
CEM III/B - 10%
CEM III/B - 5%
Normalized G0
Time (days)


(b)

FIGURE 8

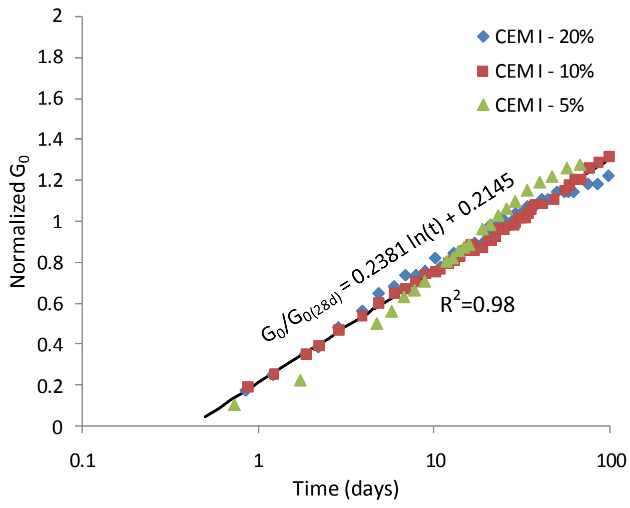

CEM I - 20%
CEM I - 10%
CEM I - 5%
$G_0/G_{0(28d)} = 0.2381 \ln(t) + 0.2145$
$R^2=0.98$
Normalized $G_0$
Time (days)


(a)

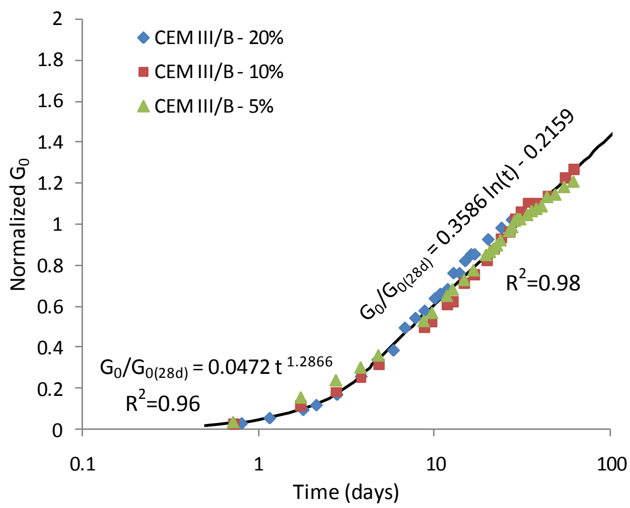

CEM III/B - 20%
CEM III/B - 10%
CEM III/B - 5%
$G_0/G_{0(28d)} = 0.3586 \ln(t) - 0.2159$
$R^2=0.98$
$G_0/G_{0(28d)} = 0.0472\, t^{1.2866}$
$R^2=0.96$
Normalized $G_0$
Time (days)


(b)

FIGURE 9

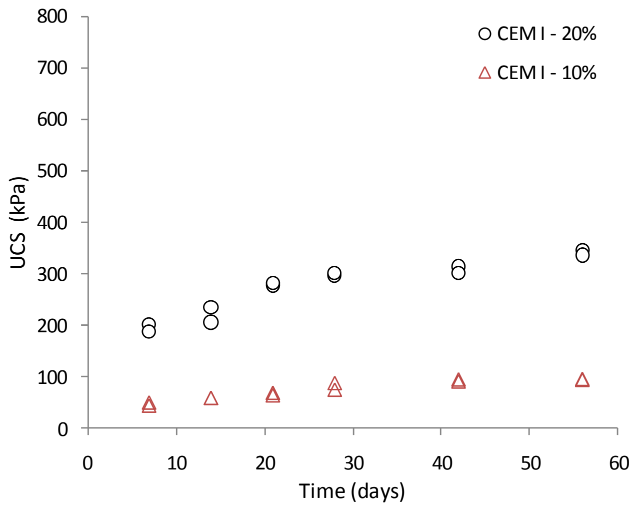

CEM I - 20%
CEM I - 10%
UCS (kPa)
800
700
600
500
400
300
200
100
0
0
10
20
30
40
50
60
Time (days)


(a)

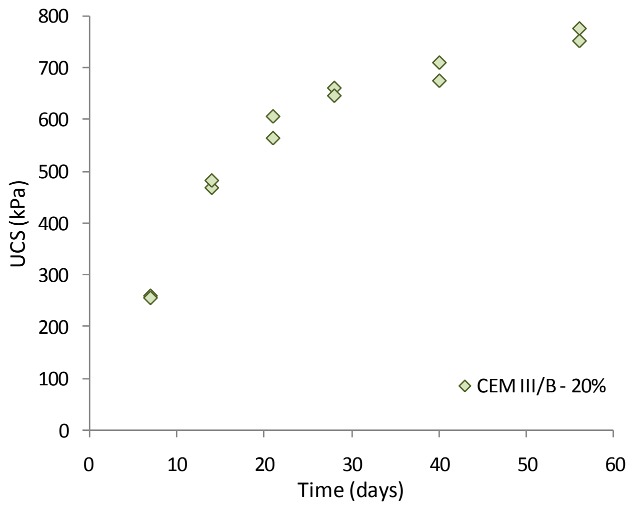

UCS (kPa)
800
700
600
500
400
300
200
100
0
CEM III/B - 20%
0
10
20
30
40
50
60
Time (days)


(b)

FIGURE 10

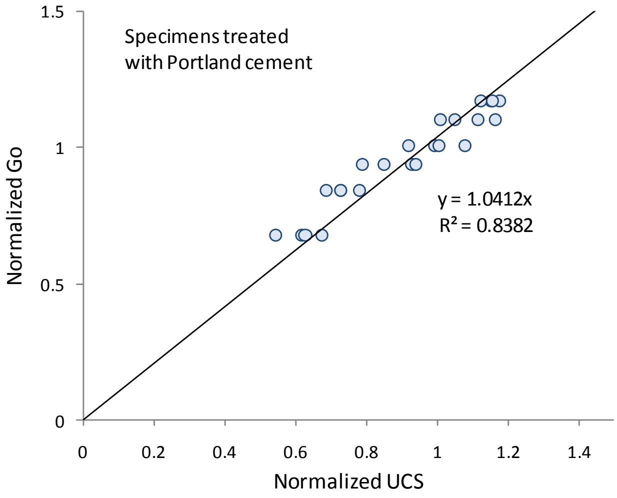

Specimens treated
with Portland cement
y = 1.0412x
R² = 0.8382
Normalized Go
Normalized UCS
0
0.5
1
1.5
0
0.2
0.4
0.6
0.8
1
1.2
1.4


(a)

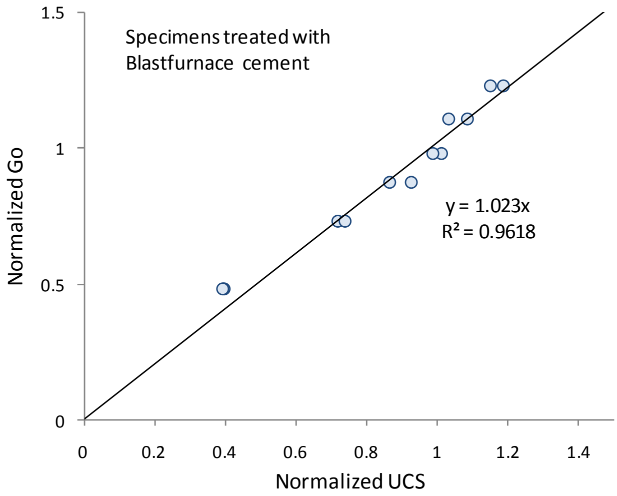

Specimens treated with
Blastfurnace cement
y = 1.023x
R² = 0.9618
Normalized Go
Normalized UCS
0
0.5
1
1.5
0
0.2
0.4
0.6
0.8
1
1.2
1.4


(b)

FIGURE 11

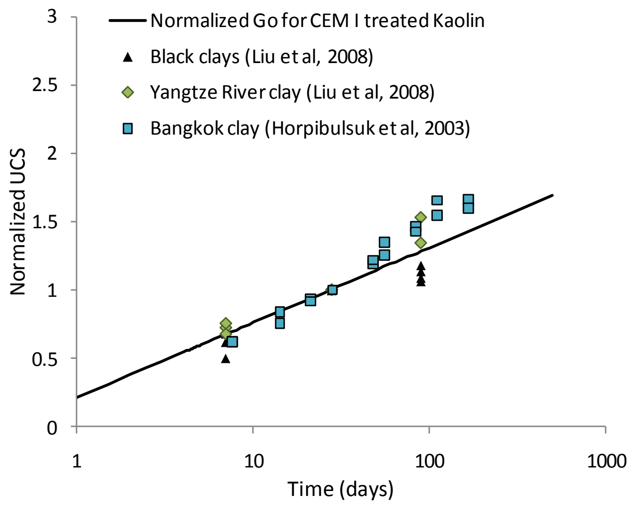

Normalized Go for CEM I treated Kaolin
Black clays (Liu et al, 2008)
Yangtze River clay (Liu et al, 2008)
Bangkok clay (Horpibulsuk et al, 2003)
Normalized UCS
Time (days)
0
0.5
1
1.5
2
2.5
3
1
10
100
1000


(a)

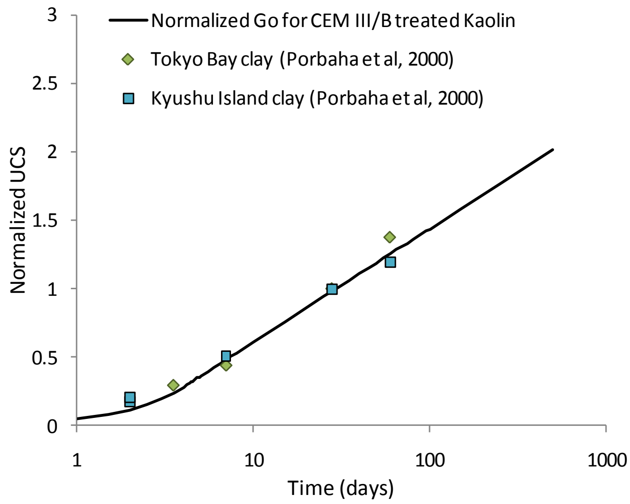

Normalized Go for CEM III/B treated Kaolin
Tokyo Bay clay (Porbaha et al, 2000)
Kyushu Island clay (Porbaha et al, 2000)
Normalized UCS
Time (days)
0
0.5
1
1.5
2
2.5
3
1
10
100
1000


(b)